

Quantitative in situ measurement of optical force along a strand of cleaved silica optical fiber induced by the light guided therewithin

Mikko Partanen,^{1,2} Hyeonwoo Lee,¹ and Kyunghwan Oh¹

¹*Photonic Device Physics Laboratory, Department of Physics, Yonsei University, 50 Yonsei-ro Seodaemun-gu, Seoul 03722, Korea*

²*Photonics Group, Department of Electronics and Nanoengineering, Aalto University, P.O. Box 15500, 00076 Aalto, Finland*

(Dated: June 7, 2021)

We proposed an optomechanical system to quantify the net force on a strand of cleaved silica optical fiber in situ as the laser light was being guided through it. Four strands of the fiber were bonded to both sides of a macroscopic oscillator, whose movements were accurately monitored by a Michelson interferometer. The laser light was propagating with variable optical powers and frequency modulations. Experimentally, we discovered that the driving force for the oscillator consisted of not only the optical force of the light exiting from the cleaved facets but also the tension along the fiber induced by the light guided therewithin. The net driving force was determined only by the optical power, refractive index of the fiber, and the speed of light, which pinpoints its fundamental origin.

In optomechanics, the motion of mechanical resonators is typically controlled by using laser light reflected from a mirror [1–7]. Therefore, the optical force, which drives these mechanical resonators is the well-known radiation pressure of light incident from free space. However, light can also exert forces while it is propagating inside materials, and in particular, when it is crossing material interfaces. Mostly, these forms of optical forces are studied in liquids by observing the deformation or movement of liquid surfaces under optical excitation [8–13]. There also exist measurements of the steady-state radiation pressure on mirrors immersed in liquids [14, 15]. Experiments on the forces of light in lossless solids have been very scarce and rather qualitative or hindered by the lossy nature of solids [16–23]. From literature, one can conclude that previous works have used neither mechanical resonators nor optical fibers to quantitatively measure optical forces inside materials. This is surprising and calls for a change since optical forces have an important role, e.g., in whispering gallery mode resonators [24, 25] and as a source of cross-talk in multi-core fibers [26].

Among solid dielectric media, silica optical fiber is considered to be de facto the lowest-loss medium with the highest uniformity along its length [27], yet the forces of light carried by the optical fiber have not been quantified in experiments yet. In this work, we proposed a macroscopic oscillator platform to interferometrically quantify the forces of light, which is being guided through a silica optical fiber, for the first time to the best knowledge of the authors. We used cleaved optical fiber strands bonded to a macroscopic oscillator to make the light propagating through the optical fiber the only driving force of the oscillator. Our platform is schematically illustrated in Fig. 1. A 3D printed mass was suspended by a spring at the center and, on both sides, the cleaved optical fibers were glued. Note that our experiment leaves no room for different interpretations of the origin of the oscillator signal but the forces of light propagating through the optical

fibers. In particular, heating effects, whose consequences in many prior cases have dominated over the optical momentum transfer, are negligible since light propagating inside a commercial multimode optical fiber less than a meter experiences a loss less than 0.002 dB. Thermal effects are also hindered by the large thermal time constant of the macroscopic oscillator [4, 28].

A 3D printed mass was designed to be held by a spring at the center and balanced by optical fiber strands glued at both ends as illustrated in Fig. 1(a). A laser was split into four strands of commercial 0.22 NA multimode optical fibers (Thorlabs, FG105LCA) with equal optical power using a 1x4 splitter. The optical fibers, with cross-section in Fig. 1(b), were cleaved at 90 degree and aligned vertically downward. To confirm the universality of our results, we studied two oscillators with different masses and damping constants, one driven at the wavelength of 808 nm and the other at 915 nm. The longitudinal displacements of the oscillators were detected by a Michelson interferometer in Fig. 1(c) using a He-Ne laser and a mirror attached at the bottom of the mass. Shifts of the interference fringes were recorded with a camera at a frame rate of 200 frames per second for various incident laser powers and modulation frequencies. A more complete description of the experiment is presented in the Supplemental Material [29].

The optical forces induced by the light guided in the optical fiber can be divided into the force at the air-silica interface of the optical fiber facet, and the tension along the fiber strands as schematically shown by $\mathbf{F}_{\text{interface}}$ and $\mathbf{F}_{\text{tension}}$ in Fig. 1(a). The force \mathbf{F} on an object is equal to the temporal change of its momentum \mathbf{p} as $\mathbf{F} = d\mathbf{p}/dt$. We study the momentum transfer of light at the end facet of optical fibers, where the light experiences the air-fiber core interface. The momentum of light in the optical fiber and the air is denoted by p , and p_0 , respectively. Then, by summing over the four fibers of Fig. 1(a), we obtain the magnitude of the total interface force from the

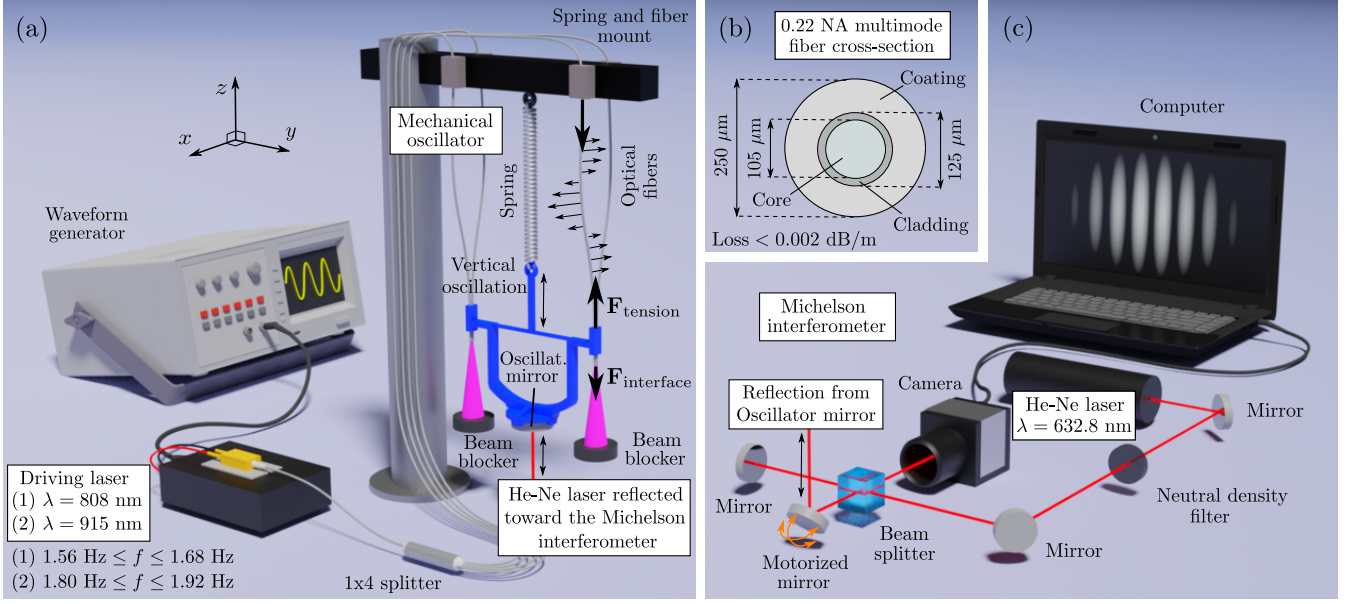


FIG. 1. (a) The mechanical oscillator was driven by optical interface forces $\mathbf{F}_{\text{interface}}$ and tension $\mathbf{F}_{\text{tension}}$ of the four fibers, where the laser was propagating. These forces, illustrated for one of the fibers, were modulated by varying the laser intensity. The wavelength was either at 808 nm or 915 nm. (b) The cross-section of the 0.22 NA multimode fiber (Thorlabs, FG105LCA). (c) The nanoscale oscillation was detected by the Michelson interferometer.

conservation law of momentum as

$$F_{\text{interface}} = \left[T - \frac{p}{p_0}(1 + R) \right] \frac{P}{c}. \quad (1)$$

Positive and negative values of $F_{\text{interface}}$ indicate whether the force is upward or downward in Fig. 1(a), respectively, and $P = \sum_{i=1}^4 P_i$ is the sum of the incident optical powers of the four fibers. The power reflection coefficient R , and the power transmission coefficient $T = 1 - R$ are equal in the four fibers. For the cleaved fiber facet without any thin-film coating, R and T are given by Fresnel formulas as $R = [(n - 1)/(n + 1)]^2$ and $T = 4n/(n + 1)^2$. Here n is the refractive index of the fiber core and we set the refractive index of air to unity.

When light propagates along a bent fiber, the optical force pushes the fiber walls unequally at different sides and the net momentum flux of light changes its direction. This is a direct consequence of the momentum conservation law. The optical force on the fiber walls points in the direction of the positive curvature, which is always normal to the fiber as indicated by the small arrows in Fig. 1(a). From the elasticity theory (see the Supplemental Material [29]), it follows that this normal force gives rise to tension in the longitudinal direction of the fiber. The net tension of the four fibers is given by

$$F_{\text{tension}} = \sum_{i=1}^4 \int_{A_i} (T_{zz,i} - T_{zz,i}^{(0)}) dxdy = \frac{p}{p_0}(1 + R) \frac{P}{c}. \quad (2)$$

Here $T_{zz,i}$ is the diagonal component of the stress tensor of the fiber i in the vertical direction when the light

is guided through of the fiber, $T_{zz,i}^{(0)}$ is the stress tensor component in the absence of the light, and A_i is the total cross-sectional area of the fiber i on the side of the oscillator.

From the optical interface force in Eq. (1) and the tension along fibers in Eq. (2), the net time-dependent driving force of the mechanical oscillator is given by

$$F = F_{\text{interface}} + F_{\text{tension}} = \frac{TP}{c}. \quad (3)$$

The net force in Eq. (3) is interestingly independent of the value of the momentum of light inside the fiber since the dependence on p is canceled out. It is, however, seen that this net force depends only on the optical power, refractive index of the fiber, and the speed of light, which pinpoints its fundamental origin.

For the mechanical oscillator used to detect the net laser-induced force, we write Newton's equation of motion as [30]

$$\frac{d^2 z}{dt^2} + 2\zeta\omega_0 \frac{dz}{dt} + \omega_0^2 z = \frac{F}{m}, \quad (4)$$

where m is the effective mass of the oscillator, ω_0 is the undamped resonance frequency, ζ is the damping coefficient, and F is the net driving force in Eq. (3). The mechanical Q factor is defined in terms of the damping coefficient as $Q = 1/(2\zeta)$. As the mass of the vertically aligned spring is not negligible, the effective mass of the oscillator is given by Rayleigh's value $m = m_0 + m_s/3$, where m_0 is the mass of the oscillator and m_s is the mass of the spring [31].

The net force due to a laser beam harmonically modulated with angular frequency ω is denoted by $F = F_0 \cos^2(\frac{1}{2}\omega t) = \frac{1}{2}F_0[1 + \cos(\omega t)]$, where F_0 is the peak to peak force amplitude. The steady-state solution of Eq. (4) is given by $z(t) = z(\omega) \cos(\omega t + \varphi) + F_0/(2m\omega_0^2)$, where the displacement amplitude is

$$z(\omega) = \frac{F_0/m}{2\sqrt{(2\omega\omega_0\zeta)^2 + (\omega^2 - \omega_0^2)^2}} \quad (5)$$

and $\varphi = \arctan[2\omega\omega_0\zeta/(\omega^2 - \omega_0^2)] \in [-\pi, 0]$. The resonance frequency of the underdamped oscillator with $\zeta < 1/\sqrt{2}$ is $\omega_r = \omega_0\sqrt{1 - 2\zeta^2}$. At ω_r , the displacement amplitude of the oscillator in Eq. (5) obtains its peak value, $z_0 = F_0/(4m\omega_0^2\zeta\sqrt{1 - \zeta^2})$. By measuring the peak value of the displacement amplitude, one then obtains the driving force amplitude as

$$F_0 = 4m\omega_0^2\zeta\sqrt{1 - \zeta^2}z_0. \quad (6)$$

Here ω_0 and ζ can be accurately determined from the position and width of the mechanical resonance peak, and m can be obtained from the oscillator, spring, and fiber masses measured with a digital scale [28]. For our heavier oscillator, driven with the 808 nm laser, $m = (18.363 \pm 0.001)$ g, while for the lighter oscillator, driven with the 915 nm laser, $m = (16.485 \pm 0.001)$ g.

The refractive index of the pure silica core of the fiber is $n = 1.453$ at 808 nm and $n = 1.452$ at 915 nm [32]. Then, at normal incidence, the transmission coefficient for the end interface of the fiber is $T = 0.9659$ at 808 nm and $T = 0.9660$ at 915 nm. For the 0.22 NA multimode fiber, the maximum angle of incidence in the fiber is near 8.7 degrees for both wavelengths. The non-normal angles of incidence are accounted for in the analysis, even though their effect is small.

Figure 2 presents the experimental results. In Fig. 2(a), the measured displacement amplitude of the first oscillator driven at 808 nm is plotted as a function of the modulation frequency of the driving laser field. Fig. 2(b) presents the same plot for the second oscillator driven at 915 nm. The net peak to peak power amplitude of the four fibers used in these plots is $P_0 = 5.125$ W. The measurement time is an integer multiple of the modulation period close to 1000 s and the ensemble averaging is made over 10 or more measurements. As the error of the displacement amplitude, we use the standard deviation of the ensemble average.

In Figs. 2(a) and 2(b), one can see that the fitted harmonic oscillator response function of Eq. (5) accurately describes the experimental results of both oscillators. One can also observe the mechanical resonance peak in the noise spectrum that appears below the fitted response function. In the presence of photothermal effects, the response function would be modified from the ideal harmonic oscillator form as described, e.g., in Refs. [4, 33]. In accordance with the results for the free

space laser driven oscillator in Ref. [28], the photothermal effects are determined to be negligible for our macroscopic oscillator.

The fitting of the harmonic oscillator response function in the experimental data of the first oscillator in Fig. 2(a) gives the undamped frequency of the oscillator equal to $f_0 = (1.622411 \pm 0.000088)$ Hz. The damping constant and the Q-factor are found to be $\zeta = 0.002485 \pm 0.000063$ and $Q = 201.2 \pm 5.1$. The errors indicate the 68.27% confidence intervals of the fitting process corresponding to one standard deviation of normally distributed quantities. The corresponding fitting using the experimental data of the second oscillator in Fig. 2(b) gives the undamped oscillator frequency equal to $f_0 = (1.851847 \pm 0.000075)$ Hz and the damping constant equal to $\zeta = 0.003690 \pm 0.000051$, which corresponds to $Q = 135.5 \pm 1.9$.

Figures 2(c) and 2(d) present the measured peak to peak force amplitudes of the two oscillators following from Eq. (6) as a function of the peak to peak laser power amplitude. The slope of the regression line of the first oscillator is $dF_0/dP_0 = (3.28 \pm 0.10) \times 10^{-9}$ s/m = $(0.982 \pm 0.034)/c$. The relative error is 3.5%, from which 2.1% comes from the determination of the damping constant and 1.4% from the peak displacement amplitude. For the second oscillator, $dF_0/dP_0 = (3.21 \pm 0.10) \times 10^{-9}$ s/m = $(0.963 \pm 0.030)/c$. The relative error is 3.2%, from which 1.2% comes from the determination of the damping constant and 2.0% from the peak displacement amplitude. The slope of the theoretical line from Eq. (3) is $T/c = 3.22 \times 10^{-9}$ s/m = $0.966/c$. Thus, the experimental results of both oscillators agree with the theory within the experimental accuracy. Figures 2(c) and 2(d) also show that the results cannot be explained solely in terms of the interface forces of the conventional Minkowski ($p = np_0$) and Abraham ($p = p_0/n$) momentum models with Eq. (1) [34–51]. Thus, accounting for the tension in Eq. (2) is necessary, in which case both conventional models give the same net force. The appearance of more than one force component in experimental setups can partly explain how the Abraham-Minkowski controversy has continued to this day.

To the best knowledge of the authors, the only previous measurement of forces of light exiting a solid medium is She's *et al.* report [18]. In their measurements, She *et al.* were able to detect the recoil of a thin silica filament at the end where the light exited, but the results were not quantitatively accurate and their interpretation has raised subsequent debates [22, 23]. In contrast, the present work can explain the observations of She *et al.* independently of the Abraham and Minkowski momentum models by including the tension in the fiber induced by the light guided therewithin. A small bending of the filament before its end due to any asymmetry causes the light to create tension, which results in the net pushing effect on the end facet of the filament.

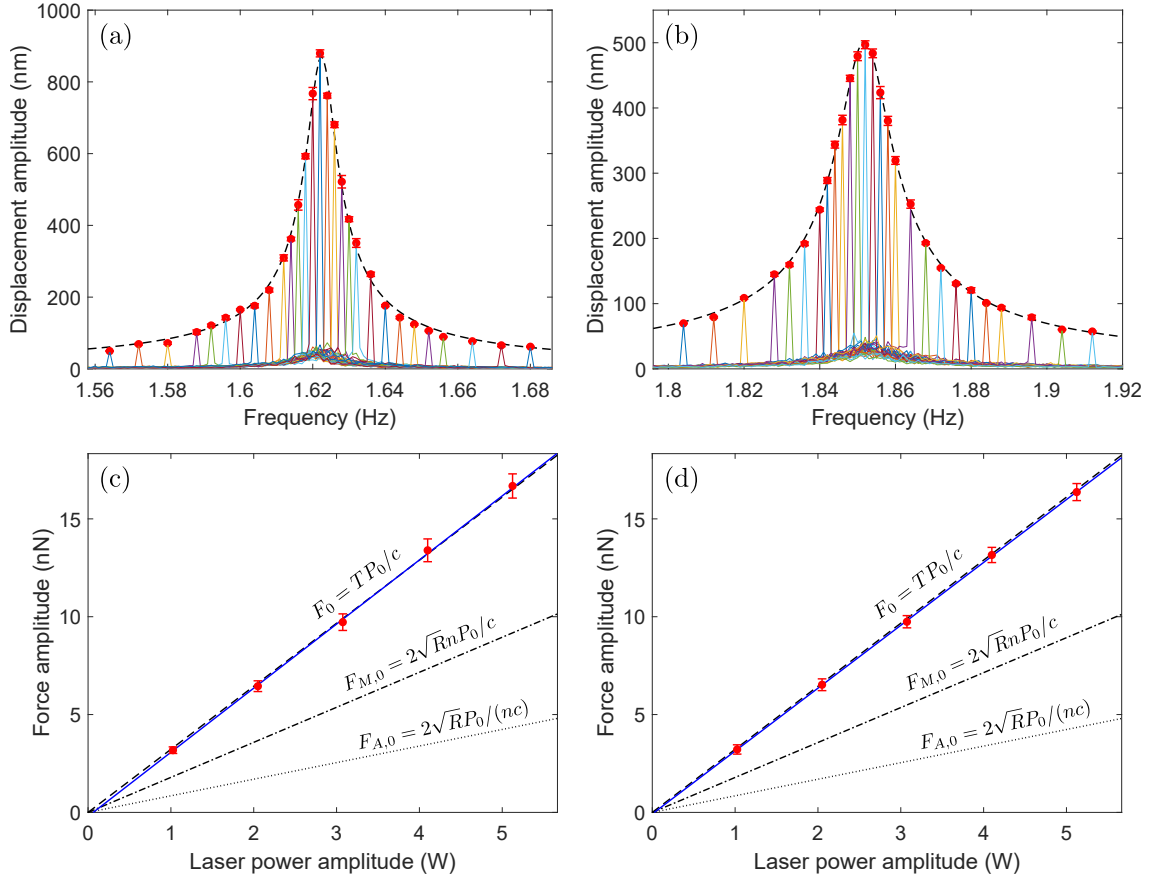


FIG. 2. The displacement amplitude of the mechanical oscillator is plotted as a function of the laser modulation frequency at the wavelength of (a) 808 nm and (b) 915 nm. The net peak-to-peak power amplitude of the driving field in the four fibers together is $P_0 = 5.125$ W in both cases. The solid line represents the averaged frequency spectrum measured with a single modulation frequency. The peak at each modulation frequency is marked with a red dot. The oscillator response function is fitted and shown by the dashed line. The corresponding peak-to-peak force amplitudes of the two oscillators are plotted in (c) and (d) as a function of the peak-to-peak laser power amplitude of the fibers r . The solid lines represent the regression lines and the dashed lines show the net theoretical force in Eq. (3). The dash-dotted and dotted lines are the results of the Minkowski ($F_{M,0}$) and Abraham ($F_{A,0}$) momentum models, respectively, using Eq. (1) with the corresponding momentum of light and excluding the tension in Eq. (2).

In conclusion, we have demonstrated that optical forces of light in an optical fiber can be quantitatively measured in situ while the fiber guides the light. We proposed an optomechanical system where a macroscopic mechanical oscillator was driven only by the optical force in the fiber and its nanoscopic displacements were monitored interferometrically. The light guided along an optical fiber provided two forces, the interface force at the end facet and the tension on a curvature. The theoretical model agreed with the experimental measurements with an accuracy of 3.5%. Our work can pave the way to more extensive use of novel mechanical resonator geometries for accurately detecting optical forces in solids, e.g., by utilizing whispering gallery modes [25].

This work has been funded by European Union's Horizon 2020 Marie Skłodowska-Curie Actions (MSCA) individual fellowship under Contract No. 846218 and the National Research Foundation of Korea (NRF)

grant by the Korea government (MSIT) under Contract No. 2019R1A2C2011293.

-
- [1] S. Gigan, H. R. Böhm, M. Paternostro, F. Blaser, G. Langer, J. B. Hertzberg, K. C. Schwab, D. Bäuerle, M. Aspelmeyer, and A. Zeilinger, "Self-cooling of a micromirror by radiation pressure," *Nature* **444**, 67 (2006).
 - [2] D. Kleckner and D. Bouwmeester, "Sub-kelvin optical cooling of a micromechanical resonator," *Nature* **444**, 75 (2006).
 - [3] D. M. Weld and A. Kapitulnik, "Feedback control and characterization of a microcantilever using optical radiation pressure," *Appl. Phys. Lett.* **89**, 164102 (2006).
 - [4] D. Ma, J. L. Garrett, and J. N. Munday, "Quantitative measurement of radiation pressure on a microcantilever in ambient environment," *Appl. Phys. Lett.* **106**, 091107 (2015).

- [5] D. R. Evans, P. Tayati, H. An, P. K. Lam, V. S. J. Craig, and T. J. Senden, "Laser actuation of cantilevers for picometre amplitude dynamic force microscopy," *Sci. Rep.* **4**, 5567 (2014).
- [6] R. Wagner, F. Guzman, A. Chijioke, G. K. Gulati, M. Keller, and G. Shaw, "Direct measurement of radiation pressure and circulating power inside a passive optical cavity," *Opt. Express* **26**, 23492 (2018).
- [7] P. R. Wilkinson, G. A. Shaw, and J. R. Pratt, "Determination of a cantilever's mechanical impedance using photon momentum," *Appl. Phys. Lett.* **102**, 184103 (2013).
- [8] N. G. C. Astrath, L. C. Malacarne, M. L. Baesso, G. V. B. Lukasiewicz, and S. E. Bialkowski, "Unravelling the effects of radiation forces in water," *Nat. Commun.* **5**, 4363 (2014).
- [9] A. Ashkin and J. M. Dziedzic, "Radiation pressure on a free liquid surface," *Phys. Rev. Lett.* **30**, 139 (1973).
- [10] A. Casner and J.-P. Delville, "Giant deformations of a liquid-liquid interface induced by the optical radiation pressure," *Phys. Rev. Lett.* **87**, 054503 (2001).
- [11] H. Choi, M. Park, D. S. Elliott, and K. Oh, "Optomechanical measurement of the Abraham force in an adiabatic liquid-core optical-fiber waveguide," *Phys. Rev. A* **95**, 053817 (2017).
- [12] F. A. Schaberle, L. A. Reis, C. Serpa, and L. G. Arnaut, "Photon momentum transfer at water/air interfaces under total internal reflection," *New J. Phys.* **21**, 033013 (2019).
- [13] L. Zhang, W. She, N. Peng, and U. Leonhardt, "Experimental evidence for Abraham pressure of light," *New J. Phys.* **17**, 053035 (2015).
- [14] R. V. Jones and J. C. S. Richards, "The pressure of radiation in a refracting medium," *Proc. R. Soc. Lond. A* **221**, 480 (1954).
- [15] R. V. Jones and B. Leslie, "The measurement of optical radiation pressure in dispersive media," *Proc. R. Soc. Lond. A* **360**, 347 (1978).
- [16] A. Kundu, R. Rani, and K. S. Hazra, "Graphene oxide demonstrates experimental confirmation of Abraham pressure on solid surface," *Sci. Rep.* **7**, 42538 (2017).
- [17] A. F. Gibson, M. F. Kimmitt, and A. C. Walker, "Photon drag in germanium," *Appl. Phys. Lett.* **17**, 75 (1970).
- [18] W. She, J. Yu, and R. Feng, "Observation of a push force on the end face of a nanometer silica filament exerted by outgoing light," *Phys. Rev. Lett.* **101**, 243601 (2008).
- [19] I. Brevik, "Analysis of recent interpretations of the Abraham-Minkowski problem," *Phys. Rev. A* **98**, 043847 (2018).
- [20] M. Partanen and J. Tulkki, "Comment on 'Analysis of recent interpretations of the Abraham-Minkowski problem'," *Phys. Rev. A* **100**, 017801 (2019).
- [21] I. Brevik, "Reply to 'Comment on 'Analysis of recent interpretations of the Abraham-Minkowski problem''," *Phys. Rev. A* **100**, 017802 (2019).
- [22] I. Brevik, "Comment on 'Observation of a push force on the end face of a nanometer silica filament exerted by outgoing light'," *Phys. Rev. Lett.* **103**, 219301 (2009).
- [23] M. Mansuripur, "Comment on 'Observation of a push force on the end face of a nanometer silica filament exerted by outgoing light'," *Phys. Rev. Lett.* **103**, 019301 (2009).
- [24] A. Schliesser, G. Anetsberger, R. Rivière, O. Arcizet, and T. J. Kippenberg, "High-sensitivity monitoring of micromechanical vibration using optical whispering gallery mode resonators," *New J. Phys.* **10**, 095015 (2008).
- [25] I. Brevik and S. A. Ellingsen, "Possibility of measuring the Abraham force using whispering gallery modes," *Phys. Rev. A* **81**, 063830 (2010).
- [26] H. H. Diamandi, Y. London, and A. Zadok, "Optomechanical inter-core cross-talk in multi-core fibers," *Optica* **4**, 289 (2017).
- [27] K. Oh and U.-C. Paek, *Silica Optical Fiber Technology for Devices and Components: Design, Fabrication, and International Standards*, Wiley, Hoboken, NJ (2012).
- [28] M. Partanen, H. Lee, and K. Oh, "Radiation pressure measurement using a macroscopic oscillator in an ambient environment," *Sci. Rep.* **10**, 20419 (2020).
- [29] See Supplemental Material at (link to be provided by editors) for a more detailed description of the experiment.
- [30] M. Aspelmeyer, T. J. Kippenberg, and F. Marquardt, "Cavity optomechanics," *Rev. Mod. Phys.* **86**, 1391 (2014).
- [31] W. T. Thomson and M. Dahleh, *Theory of Vibration with Applications*, Prentice-Hall, New Jersey (1998).
- [32] I. H. Malitson, "Interspecimen comparison of the refractive index of fused silica," *J. Opt. Soc. Am.* **55**, 1205 (1965).
- [33] D. Ma and J. N. Munday, "Measurement of wavelength-dependent radiation pressure from photon reflection and absorption due to thin film interference," *Sci. Rep.* **8**, 15930 (2018).
- [34] M. Abraham, "Zur Elektrodynamik bewegter Körper," *Rend. Circ. Matem. Palermo* **28**, 1 (1909).
- [35] M. Abraham, "Sull'elettrodinamica di Minkowski," *Rend. Circ. Matem. Palermo* **30**, 33 (1910).
- [36] H. Minkowski, "Die Grundgleichungen für die elektromagnetischen Vorgänge in bewegten Körpern," *Nachr. Ges. Wiss. Göttin Math.-Phys. Kl.* 53 (1908), reprinted in *Math. Ann.* **68**, 472 (1910).
- [37] U. Leonhardt, "Momentum in an uncertain light," *Nature* **444**, 823 (2006).
- [38] R. N. C. Pfeifer, T. A. Nieminen, N. R. Heckenberg, and H. Rubinsztein-Dunlop, "Colloquium: Momentum of an electromagnetic wave in dielectric media," *Rev. Mod. Phys.* **79**, 1197 (2007).
- [39] S. M. Barnett, "Resolution of the Abraham-Minkowski dilemma," *Phys. Rev. Lett.* **104**, 070401 (2010).
- [40] S. M. Barnett and R. Loudon, "The enigma of optical momentum in a medium," *Phil. Trans. R. Soc. A* **368**, 927 (2010).
- [41] M. Partanen, T. Häyrynen, J. Oksanen, and J. Tulkki, "Photon mass drag and the momentum of light in a medium," *Phys. Rev. A* **95**, 063850 (2017).
- [42] K. Y. Bliokh, A. Y. Bekshaev, and F. Nori, "Optical momentum, spin, and angular momentum in dispersive media," *Phys. Rev. Lett.* **119**, 073901 (2017).
- [43] K. Y. Bliokh, A. Y. Bekshaev, and F. Nori, "Optical momentum and angular momentum in complex media: from the Abraham-Minkowski debate to unusual properties of surface plasmon-polaritons," *New J. Phys.* **19**, 123014 (2017).
- [44] M. Partanen and J. Tulkki, "Mass-polariton theory of light in dispersive media," *Phys. Rev. A* **96**, 063834 (2017).
- [45] B. A. Kemp, "Resolution of the Abraham-Minkowski debate: Implications for the electromagnetic wave theory of light in matter," *J. Appl. Phys.* **109**, 111101 (2011).
- [46] M. Partanen and J. Tulkki, "Lorentz covariance of the

- mass-polariton theory of light,” *Phys. Rev. A* **99**, 033852 (2019).
- [47] M. Partanen and J. Tulkki, “Lagrangian dynamics of the coupled field-medium state of light,” *New J. Phys.* **21**, 073062 (2019).
 - [48] U. Leonhardt, “Abraham and Minkowski momenta in the optically induced motion of fluids,” *Phys. Rev. A* **90**, 033801 (2014).
 - [49] P. W. Milonni and R. W. Boyd, “Momentum of light in a dielectric medium,” *Adv. Opt. Photon.* **2**, 519 (2010).
 - [50] I. Brevik, “Experiments in phenomenological electrodynamics and the electromagnetic energy-momentum tensor,” *Phys. Rep.* **52**, 133 (1979).
 - [51] M. Partanen and J. Tulkki, “Light-driven mass density wave dynamics in optical fibers,” *Opt. Express* **26**, 22046 (2018).